Estimation of Convection Loss from Paraboloidal Dish Cavity Receivers

S. Paitoonsurikarn, T. Taumoefolau and K. Lovegrove
Centre for Sustainable Energy Systems,
Department of Engineering,
Australian National University,
Canberra ACT 0200,
AUSTRALIA
E-mail: sawat.paitoonsurikarn@anu.edu.au

Abstract

In general, cavity receivers employed in the sun-tracking paraboloidal dish concentrator are subjected to various modes of heat loss. Among these, convection is the most complicated phenomenon and yet also a major contributor of the total energy loss. Hence, its characteristics need to be clarified such that it can be effectively minimized for the improvement of system efficiency. This study undertakes the numerical investigation of natural and combined convection loss from cavity receivers employed in solar paraboloidal dishes. Three different receiver geometries have been considered. One of these is the experimental model receiver for validating the numerical results. The other two are essentially the ones currently used in ANU 20 m^2 and 400 m^2 dishes. For natural convection study, two simple models that can estimate heat loss with reasonable accuracy are proposed.

On the combined convection loss study, several cases of varying wind speeds and directions are considered and some typical results are presented in graphical form. They clearly show a general relationship of wind characteristics and heat loss. The range of wind speed in which force convection dominates can be clarified.

1. INTRODUCTION

Convective heat transfer is a significant source of energy loss from thermal receivers used with dish solar concentrators. This paper presents new results from an investigation of natural and combined convection heat transfer from open cavity receivers employed in sun-tracking paraboloidal dish applications. These results continue an investigation that was reported at Solar 2003 (Paitoonsurikarn & Lovegrove, 2003). The experimental and numerical investigation of natural convection heat transfer has also been published in Taumoefolau e*t a*l (2004).

Three different cavity geometries have been considered. One of these is an experimental model receiver used for validating the numerical results in Taumoefolau e*t a*l (2004). The other two are the ones currently used in ANU 20 m^2 and 400 m^2 dishes. In the topic of natural convection, the parametric study of heat loss by varying relevant parameters, i.e., cavity size, aspect ratio, and wall temperature which have not been investigated in the preceding work has been carried out. The objective was to use the results to further improve the validity of the previously-proposed correlation equation for heat loss (Paitoonsurikarn & Lovegrove, 2003). The newly-developed correlation based on modified Stine & McDonald model (Leibfried & Ortjohann, 1995) is also proposed herein.

In the topic of combined free-forced convection, i.e. that includes the effect of wind speed and direction on convection loss, several additional cases to those presented in the preceding work have been undertaken. In particular, several cases of varying wind incident angles are considered and some typical results are summarized in graphical form.

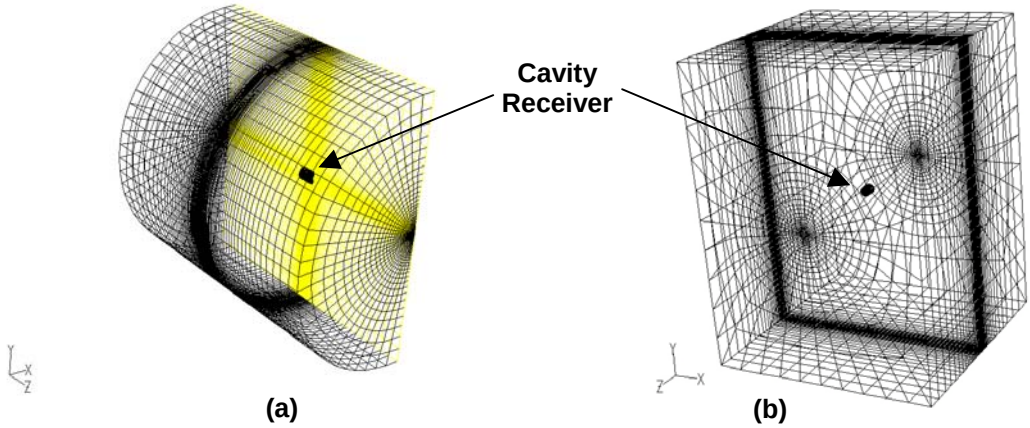

Figure 1 (a) Old and (b) New Grid Structures for Natural Convection Study.

2. NUMERICAL PROCEDURE

The commercial CFD software package, Fluent 6.0 (Fluent Inc., 2002), is employed in the 3D simulation of both natural and combined convection. Problem formulation and the boundary conditions used for each study are described below.

2.1. Natural Convection

In all simulations, the receiver is assumed to be placed in a "virtual enclosure" sufficiently large to approximate the behavior of an infinite flow field. The present work employs new grids in which the computational extent is equal to the full physical domain of the flow system in order to take into account any possible asymmetry of flow and temperature fields. In the previously published work, contrarily, grids cover only one half on the assumption that the flow field should be symmetric. The new and old grid structures are shown together in Figure 1. The other major improvement of the new grid is that it has a smaller total number of cells by having the bigger cell size of every cell away from the receiver. This significantly reduces the computational time needed for one simulation. The results of convection loss calculated from old and new grids show quite a good agreement with each other. This indicates that the symmetrical assumption used in the old grid was reasonable. Also, the new grid can be used with confidence.

For boundary conditions, the enclosure wall is set to ambient temperature of 27^{o}C. The receiver's cavity and outer walls are assumed to be isothermal and adiabatic, respectively. The cavity wall temperature is set arbitrarily.

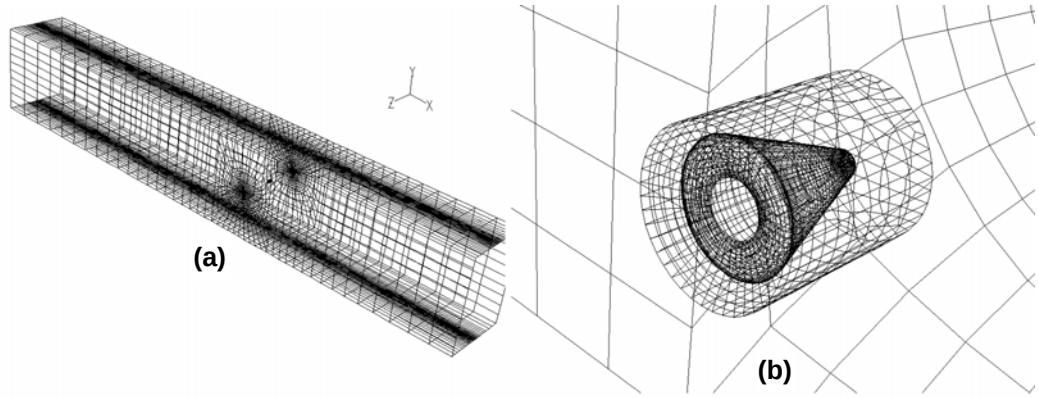

Figure 2 Typical Grid of Combined Convection Study for the case of 20 m^2 Solar Dish Receiver with Wind Parallel to the Aperture Plane; (a) Wind Tunnel Structure, (b) Receiver Close up.

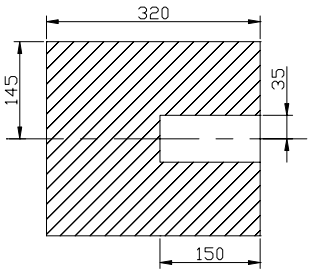

Figure 3 Drawing of the Model Receiver. Dimension Shown in mm.

2.2. Combined Convection

For combined convection, the receiver is modeled as if it is located in the center of a very long wind tunnel of rectangular cross section. A typical grid is shown in Figure 2. Wind incident angle upon the receiver is adjusted by changing the receiver's orientation.

The temperatures of the incoming airflow and the tunnel wall were set at an ambient temperature of 27°C. As with natural convection simulation, the receiver outer wall is assumed to be adiabatic, and the cavity wall temperature is set to values of interest.

More details of the numerical procedure for both natural and combined convection studies can be found in the previous paper (Paitoonsurikarn & Lovegrove, 2003). Most of the present simulations are carried out on the model receiver due to its simplest geometry which helps clarifying the effect of each parameter under study. Its relevant dimension is shown in Figure 3.

3. RESULTS AND DISCUSSION

3.1. Natural Convection

The effects of cavity size, cavity wall temperature (T_w), and cavity aspect ratio (Ar) on convection heat flux from cavity wall are shown in Figures 4-6, respectively. Figure 4 shows the convection heat flux versus the cavity inclination (θ) for various cavity sizes. The trace with label "original" corresponds to the real size of model receiver used in the experiment. It is obvious that wall heat fluxes from all cavities with up to six times bigger sizes than the original's show quite similar values over the entire range of cavity inclination. This indicates that the convection heat flux is not strongly related to the

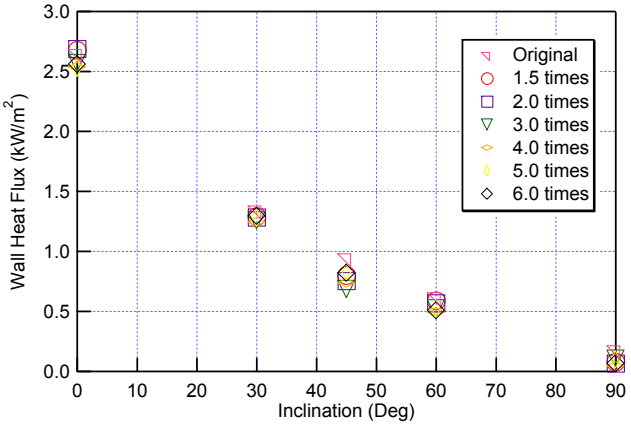

Figure 4 Effect of Cavity Size for the Case of Model Receiver. T_w=715.6 K.

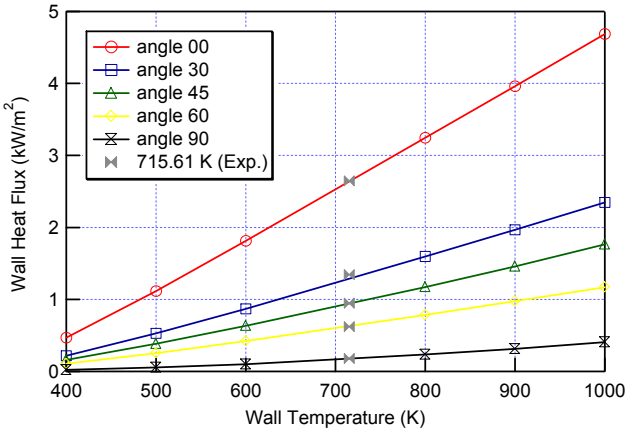

Figure 5 Effect of Cavity Wall Temperature (T_w) for the Case of Model Receiver.

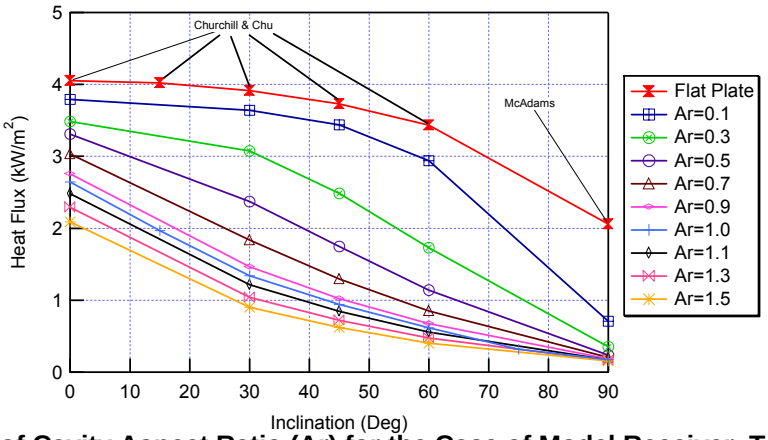

Figure 6 Effect of Cavity Aspect Ratio (Ar) for the Case of Model Receiver. T_w=715.6 K.

cavity size. In other word, the convection heat loss from any receivers is direct proportional to their cavity wall area if those receivers have similar geometry and under the same operating condition.

Figure 5 shows the convection heat flux versus cavity wall temperature (T_w) at various cavity inclinations along with the experimental result. It is evident that the heat flux is very close to linearly dependent on T_w. The slope of the functional relationship between the two, however, depends on the inclination. The very good agreement between numerical and the experimental results obtained at 715.61 K is apparent.

Figure 6 shows the convection heat flux versus the cavity inclination for various cavity aspect ratios. The aspect ratio (Ar) is simply defined by the ratio of cavity depth to average diameter. The Ar values shown are further normalized by the original value of 2.21. The limiting case of a flat plate representing a cavity with zero Ar is calculated by using two empirical correlations. For $0^o \le \theta \le 60^o$, the correlation proposed by Churchill & Chu (1975) for vertical flat plate is used with cosine multiplied to the gravitational constant to take into account the inclination effect. For $\theta=90^o$, the correlation for horizontal flat plate proposed by McAdam (1954) is employed. Figure 6 clearly illustrates that heat flux increases with decreasing Ar, i.e., with shallower cavity. The numerical solution tends to approach the flat plate values. Change of the curvature from the bottom trace (Ar=1.5) to the top trace (Ar=0.1) is noticeable.

In the previous work (Paitoonsurikarn & Lovegrove, 2003), a semi-empirical correlation for the heat transfer coefficient (h) that can be employed in the estimation of the convection heat loss from the open cavity receiver was developed in the form:

$$Nu = C \cdot Ra^n, \tag{1}$$

where Nusselt number (Nu) is a non-dimensional heat transfer coefficient = $h \cdot L_s/k$. k is the conductivity of the fluid. L_s is the characteristic length of the flow situation. . The Rayleigh number (Ra) is defined by:

$$Ra = \frac{g\beta\Delta T L_s^3}{\upsilon\alpha}, \tag{2}$$

where g is the gravitational constant, ΔT is the relevant temperature difference. β, υ,and α are the thermal expansion coefficient, kinematic viscosity, and thermal diffusivity of the fluid, respectively. The two constants C and n in Equation (1) were found to be 0.00324 and 0.447, respectively.

It was found out that the cavity length scale (L_s) is dependent on average cavity diameter D_{cav}, aperture diameter D_{ap}, cavity depth L, and sine and cosine of the inclination angle θ. It yields the following expression:

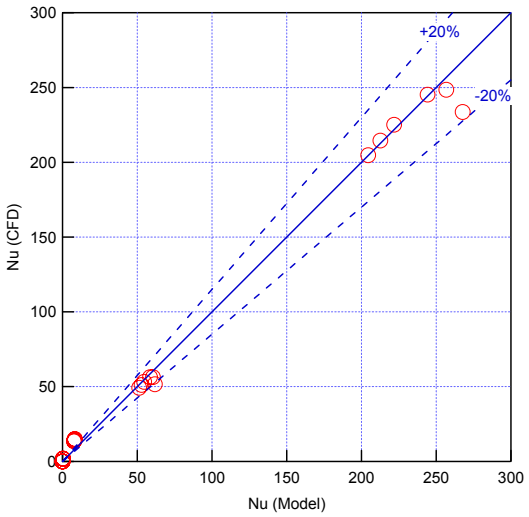

Figure 7 Comparison of Nusselt Numbers Obtained from Numerical Result and Model.

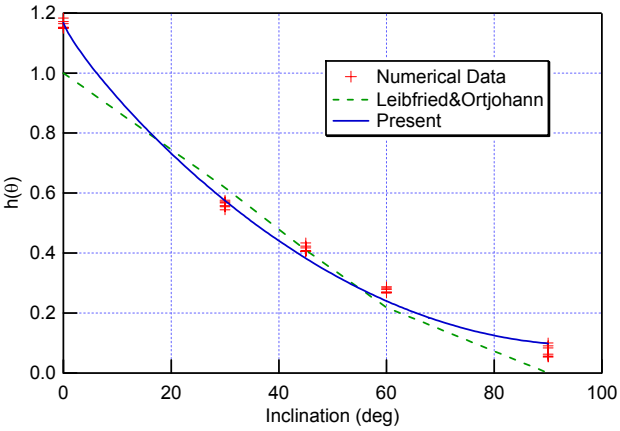

Figure 8 Comparison of Angle Dependent Functions.

$$L_s = \left(4.79\cos^{4.43}(\theta) - 0.37\sin^{0.719}(\theta)\right)D_{cav} + \left(1.06\cos^{3.24}(\theta) - 0.0462\sin^{0.286}(\theta)\right)D_{ap} + \left(7.07\cos^{5.31}(\theta) + 0.221\sin^{2.43}(\theta)\right)L\,. \quad (3)$$

Equation (1) correlates the previous numerical results for all cavity geometries quite well. However, it fails to predict the newly obtained results with varying wall temperature (T_w). Reminding that, the above model was derived from the numerical results of three cavity receivers with only one T_w considered in each case. An adjustment can be made by redefining C and n in Equation (1) as functions of T_w as follows:

$$C = 8.2066e-06 \cdot \left(\frac{T_w}{T_{amb}}\right)^{2.5837}, \text{ and} \quad (4)$$

$$n = 0.67824 \cdot \left(\frac{T_w}{T_{amb}}\right)^{-0.064548}, \quad (5)$$

where T_{amb} is an ambient temperature. The comparison between Nusselt Numbers obtained from several CFD simulations and from Equation (1) with C and n calculated from Equations (4) and (5) is shown in Figure 7. It confirms that the adjusted model can predict most of the numerical results within 20% accuracy except in the region of low Nu. This region essentially corresponds to the situation of the cavity inclination approaching 90°, where convection heat loss is very low.

As an alternative to the above model, the modified Stine & McDonald model proposed by Leibfried & Ortjohann (1995) can be used to estimate the natural convection loss with little modification:

$$Nu = 0.106Gr^{1/3}\left(\frac{T_w}{T_{amb}}\right)^{0.18}\left(4.256\frac{A_{ap}}{A_{cav}}\right)^{s} h(\theta), \quad (6)$$

where Grashof number (Gr) is defined by:

$$Gr = \frac{g\beta\Delta T L_s^3}{\upsilon^2}. \quad (7)$$

A_{ap} and A_{cav} are the area of cavity aperture and internal wall, respectively. The exponent s is an algebraic function of A_{ap}/A_{cav}. It yields the following form:

$$s = 0.56 - 1.01\left(\frac{A_{ap}}{A_{cav}}\right)^{1/2}. \quad (8)$$

In the context of Leibfried & Ortjohann work, the angle dependent function $h(\theta)$ is defined as a rather complicated transcendental function. However, it is found in the present work that the original definition of $h(\theta)$ does not make the model of Equation (6) matched with the numerical data well. Therefore, $h(\theta)$ has been modified to be:

$$h(\theta) = 1.1677 - 1.0762 \cdot \sin(\theta^{0.8324}), \quad (9)$$

where θ is in radian.

The comparison of old and new $h(\theta)$ models together with corresponding values obtained from the simulations are shown in Figure 8. It is clearly illustrated that the modified $h(\theta)$ of equation (9) better matches with the present result.

Both models are quite promising in the natural convection loss prediction in most cases. It is found however, that they fail to predict heat loss from shallow cavities with aspect ratio < 0.5. Nonetheless, those types of cavity rarely find use in real application.

3.2. Combined Convection

The most recent results of combined convection study are shown in Figures 9 and 10 which all represent the case of the cylindrical model receiver. Figure 9 shows the relationship of convection heat loss to wind speed with wind parallel to the aperture plane at various cavity inclinations and with wind normal to the aperture plane. For the parallel wind case, at zero inclination, i.e., a horizontal cavity, the heat loss first decreases with increasing wind speed up to about 5 m/s. Then, it starts to increase monotonically with increasing wind speed beyond that. The local minimum of heat loss at wind speed of 5 m/s is still observable at inclinations of 30° and 45°. However, this characteristic disappears at higher inclination where heat loss seems to always increase with wind speed. Heat losses from all parallel wind cases with different inclinations become indistinguishable after wind speed > 10 m/s. This implies that forced convection loss dominates in this regime.

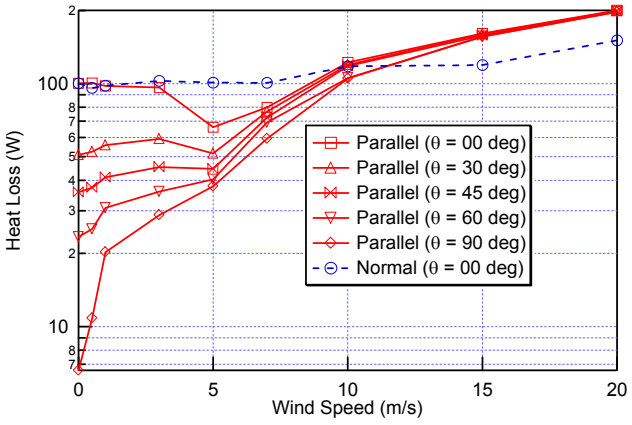

Figure 9 Heat loss versus Wind Speed for the Case of Model Receiver. T_w=715.6 K.

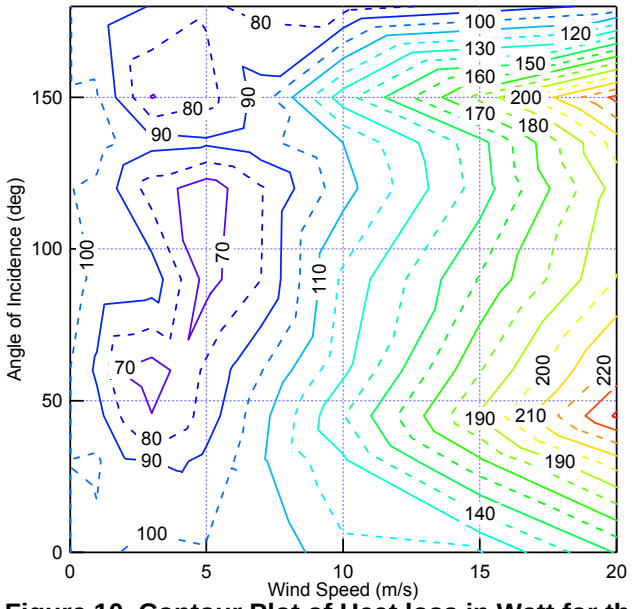

Figure 10 Contour Plot of Heat loss in Watt for the Case of Horizontal Model Receiver. T_w=715.6 K.

For the normal wind case, Figure 9 shows that heat loss does not increase much with increasing wind speed below 5 m/s, but seems to increase unboundedly with wind speed beyond that point. The explanation must presumably be related to the fact that the low wind speeds are preventing or sweeping away thermal stratification in the air and so suppressing natural convection. On the other hand, at higher wind speeds, wind starts to scour hot air from the cavity and so increases loss.

Figure 10 shows a typical contour plot of heat loss versus both wind speed and incident angle for model receiver at horizontal position. The incident angle of 0^o corresponds to the case of wind perpendicularly incident on the front of the receiver, while the angle of 90^o does to the case of wind parallel to the aperture plane. In the similar manner, the angle of 180^o corresponds to the case of wind perpendicularly incident on the back. Conforming to the above discussion, the irregular pattern of heat loss contour can be observed at low wind speed of < 10 m/s indicating the regime of equally-dominated natural and force convections. With wind speed > 10 m/s, the force convection prevails as can be seen from the well-defined pattern. The heat loss and wind speed and direction in this regime become more correlated.

4. CONCLUSION

The parametric studies of several relevant parameters in natural convection loss from open cavity receiver in solar dish application have been carried out. The previously-proposed correlation model has been modified to take into account the variation of the additional parameters. In addition, a correlation model based on the modified Stine & McDonald model is developed. Both show promising accuracy in the convection loss prediction. However, they still fail to accurately predict loss from low aspect ratio cavities. A further adjustment is needed if the loss estimation from those types of cavity is required.

More detailed investigation of combined free-forced convection has also been carried out. The effect of wind speed and direction on heat loss is clearly understood from the present result. For instance, in the case of wind parallel to the aperture plane, it is found that the buoyancy effect becomes less noticeable at high wind speed where heat loss become independent from cavity inclination and varies only with wind speed. A correlation for predicting loss in this region is a goal of the ongoing investigation.

5. REFERENCES

Churchill, S.W. and Chu H.H.S. (1975), *Correlating Equations for Laminar and Turbulent Free Convection from a Vertical Plate*, Int. J. Heat Mass Transfer 18, 1323-1329.
Fluent Inc. (2002), *Fluent 6.0 User Guide*.
Holman, J.P. (1997), *Heat transfer*. 8th edition, McGraw-Hill Companies, New York, USA.
Leibfried U. and Ortjohann J. (1995), *Convective Heat Loss from Upward and Downward-Facing Cavity Solar Receivers: Measurements and Calculations*, J. Sol. Eng. 117, 75-84.
McAdams, W.H. (1954), *Heat Transmission*. 3rd edition, McGraw-Hill Companies, New York, USA.
Paitoonsurikarn S., Lovegrove K. (2003), *On the study of Convection Loss from Open Cavity Receivers in Solar Paraboloidal Dish Application*, Proceeding of Solar 2003, ANZSES Annual Conference 2003, Melbourne, Australia.
Taumoefolau T., Paitoonsurikarn S., Hughes G., and Lovegrove K. (2004), *Experimental Investigation of Natural Convection Heat Loss from a Model Solar Concentrator Cavity Receiver*, J. Sol. Eng. 126, 801-807.